

Eclipsed M_2X_6 Compounds Exhibiting Very Short Metal–Metal Triple Bonds

David R. Manke, Zhi-Heng Loh, and Daniel G. Nocera*

Department of Chemistry, 6-335, Massachusetts Institute of Technology, 77 Massachusetts Avenue, Cambridge, Massachusetts 02139-4307

Received February 16, 2004

The preparation, characterization, and electronic structure of homoleptic complexes of molybdenum and tungsten bridged by bis(alkylamido)phenylboranes, $M_2[RN-B^{Ph}-NR]_3$ ($M = Mo$, $R = Et$ (1), iPr (2); $M = W$, $R = Et$ (3), iPr (4)), are described. These triple metal–metal bond species (i) exhibit a nearly eclipsed ligand geometry and (ii) possess the shortest metal–metal bonds of neutral dimolybdenum and ditungsten M_2X_6 complexes observed to date ($d(Mo-Mo) = 2.1612(6) \text{ \AA}$ (1); $d(W-W) = 2.2351(7) \text{ \AA}$ (4)).

Introduction

Binuclear complexes comprising d^3 metal centers are characterized by metal–metal distances of 2.2–2.4 \AA and a M_2X_6 coordination geometry in which the ligands assume an ethane-like staggered conformation.¹ The short metal–metal distance has an electronic basis that finds its origins in a bond order of three, resulting from a $\sigma^2\pi^4$ ground-state configuration. To a first approximation, this configuration precludes an electronic basis for the preferred ligand geometry. One σ and two π bonds composed of pure d_z^2 and (d_{xz} , d_{yz}) orbitals, respectively, form a cylindrically symmetric triple bond that exhibits an unrestricted barrier to rotation. The staggered conformation is presumed to arise from the reduced steric clashing of ligands across the short metal–metal bond. One bonding model modifies this description by considering the mixing of higher energy orbitals into those of the $d\sigma$ and $d\pi$ sets;² for this case, rehybridization results in greater orbital overlap between ML_3 fragments in an eclipsed ligand conformation. The preference for an eclipsed configuration vanishes when configuration interaction is included in higher order calculations.^{3–5} Nevertheless, steric factors enforce a staggered conformation in M_2X_6 complexes with monodentate ligands.⁶ An eclipsed geometry is only approached when bidentate ligands span the metal–metal

bond.^{7–12} Chisholm and Armstrong have synthesized several d^3-d^3 bimetallic compounds bridged by four-atom dianionic ligands; these compounds deviate from an eclipsed geometry by 10.7–13.9°. ^{7–11} In one case, a triple metal–metal bond species has been prepared with a bidentate ligand possessing a three-atom bridge;¹² this disiloxide-ligated complex exhibits a variance of only 3° from an eclipsed conformation.

We now report a new class of triple metal–metal bond complexes in which group 6 metals are spanned by bis(alkylamido)phenylboranes, $PhB(RN)_2^{2-}$. The three-atom bridge of this dianionic framework is structurally similar to the widely used monoanionic amidinate ligands^{13–17} with the additional feature that an electron-accepting group is situated at the bridgehead. Despite its η^2 -hapticity, the bis(alkylami-

* To whom correspondence should be addressed. E-mail: nocera@mit.edu.

- (1) Chisholm, M. H. *Acc. Chem. Res.* **1990**, *23*, 419–425.
- (2) Albright, T. A.; Hoffman, R. *J. Am. Chem. Soc.* **1978**, *100*, 7736–7737.
- (3) Hall, M. B. *J. Am. Chem. Soc.* **1980**, *102*, 2104–2106.
- (4) Cotton, F. A.; Stanley, G. G.; Kalbacher, B. J.; Green, J. C.; Seddon, E.; Chisholm, M. H. *Proc. Natl. Acad. Sci. U.S.A.* **1977**, *74*, 3109–3113.
- (5) Bursten, B. E.; Cotton, F. A.; Green, J. C.; Seddon, E. A.; Stanley, G. G. *J. Am. Chem. Soc.* **1980**, *102*, 4579–4588.

- (6) Cotton, F. A.; Walton, R. A. *Multiple Bonds between Metal Atoms*, 2nd ed.; Clarendon Press: Oxford, 1993.
- (7) Blatchford, T. P.; Chisholm, M. H.; Folting, K.; Huffman, J. C. *Inorg. Chem.* **1980**, *19*, 3175–3176.
- (8) Gilbert, T. M.; Bauer, C. B.; Bond, A. H.; Rogers, R. D. *Polyhedron* **1999**, *18*, 1293–1301.
- (9) Blatchford, T. P.; Chisholm, M. H.; Huffman, J. C. *Inorg. Chem.* **1987**, *26*, 1920–1925.
- (10) Armstrong, W. H.; Bonitatebus, P. J., Jr. *Z. Kristallogr.—New Cryst. Struct.* **1999**, *214*, 241–242.
- (11) Chisholm, M. H.; Folting, K.; Hampden-Smith, M.; Smith, C. A. *Polyhedron* **1987**, *6*, 1747–1755.
- (12) Su, K.; Tilley, T. D. *Chem. Mater.* **1997**, *9*, 588–595.
- (13) Keaton, R. J.; Jayaratne, K. C.; Henningsen, D. A.; Koterwas, L. A.; Sita, L. R. *J. Am. Chem. Soc.* **2001**, *123*, 6197–6198.
- (14) Littke, A.; Sleiman, N.; Bensimon, A. C.; Richeson, D. S. *Organometallics* **1998**, *17*, 446–451.
- (15) Chen, C.-T.; Rees, L.; Cowley, A. R.; Green, M. L. H. *J. Chem. Soc., Dalton Trans.* **2001**, 1761–1767.
- (16) Cotton, F. A.; Matusz, M.; Poli, R.; Feng, X. *J. Am. Chem. Soc.* **1988**, *110*, 1144–1154.
- (17) Chisholm, M. H.; Cotton, F. A.; Daniels, L. M.; Folting, K.; Huffman, J. C.; Iyer, S. S.; Lin, C.; Macintosh, A. M.; Murillo, C. A. *J. Chem. Soc., Dalton Trans.* **1999**, 1387–1391.

do)phenylborane ligands usually chelate a single center when interacting with main group elements.^{18–23} Only recently has the coordination chemistry of the ligand been expanded to the transition metals, but here again only for monomeric complexes.^{23–25} There are only a handful of cases in which the ligand binds two metal centers,^{21,23–27} and only one example involving a transition metal.²⁸ In this instance, the ligand assumes a $\mu\text{-}\eta^2, \eta^2$ coordination mode with both nitrogens bridging two titanium metal centers. For the triply bonded dimolybdenum and ditungsten complexes described here, the bis(alkylamido)phenylborane ligand is $\mu\text{-}\eta^1, \eta^1$. The complexes possess nearly eclipsed ligand geometries, and they are further distinguished by the shortest metal–metal distances yet observed for a neutral M_2X_6 triple metal–metal bond species. The consequences of the eclipsed geometry and short metal–metal bond on the electronic structure and reactivity of the compounds are discussed.

Experimental Section

General Procedures. All manipulations were carried out using modified Schlenk techniques under an atmosphere of N_2 or in a Vacuum Atmosphere HE-553-2 glovebox. Solvents for synthesis were of reagent grade or better and were dried according to standard methods.²⁹ Trichloro(dimethoxyethane)molybdenum(III),³⁰ bis(ethylamino)phenylborane,³¹ sodium heptachloropentakis(tetrahydrofuran)ditungstate,³² and bis(isopropylamino)phenylborane were prepared by literature methods. All other materials were used as received. *N,N'*-Dilithiobis(isopropylamido)phenylborane has been prepared previously,¹⁹ but additional analytical data for the dilithio salt is presented here. Elemental analyses were performed at H. Kolbe Mikroanalytisches Laboratorium.

PhB(EtNLi)₂·OEt₂. PhB(EtNH)₂ (500 mg) was dissolved in 7 mL of diethyl ether and frozen. Upon melting, the dropwise addition of 2.2 mL of *n*-butyllithium (2.8 M in hexanes) to the cold solution caused a white precipitate to appear after a few minutes. The room temperature mixture was stirred overnight. The fine white powder was isolated by filtration and washed with diethyl ether (3 × 5 mL) to yield 682 mg of PhB(EtNLi)₂·OEt₂ (92% yield). ¹H NMR

(300 MHz, C₆D₆, 25 °C) δ 1.000 (br s, 6H), 1.132 (t, 6H, J = 7.000 Hz), 3.021 (q, 4H, J = 6.966 Hz), 3.273 (q, 4H, J = 7.050 Hz), 7.2–7.5 (m, 5H). ¹¹B NMR (96.205 MHz, C₆D₆, 25 °C) δ 30.088. Anal. Calcd for C₁₄H₂₅BLi₂N₂O: C, 64.17; H, 9.62; N, 10.69. Found: C, 63.94; H, 9.56; N, 10.78.

PhB(ⁱPrNLi)₂. ¹H NMR (300 MHz, C₆D₆, 25 °C) δ 0.972 (d, 6H, J = 6.700 Hz), 1.097 (d, 6H, J = 7.000 Hz), 3.555 (hept, 2H, J = 6.275 Hz), 7.2–7.5 (m, 5H). ¹¹B NMR (96.205 MHz, C₆D₆, 25 °C) δ 29.580.

Mo₂[RN–B^{Ph}–NR]₃, R = Et (1) and R = ⁱPr (2). MoCl₃(dme) (100 mg) was suspended in 7 mL of toluene, and the mixture was frozen. Lithiated diamide was dissolved in toluene in a separate container; PhB(EtNLi)₂·OEt₂ (134 mg) addition gave a suspension, and PhB(ⁱPrNLi)₂ (111 mg) addition gave a solution. The desired lithiated diamide solution/suspension was added dropwise over 3 min to the partially thawed MoCl₃(dme) suspension. The resulting mixture was allowed to slowly warm to room temperature. After stirring overnight, solvent was removed by vacuum evaporation, and 10 mL of pentane was added. The solution was filtered through Celite to remove LiCl. Concentration of the solution followed by cooling to –35 °C and finally filtration afforded 28 mg of tan crystals (23.4% crystal yield) of **1** and 33 mg of tan crystals (24.3% crystal yield) of **2**. Crystals of **1** contained cocrystallized *n*-hexane; the presence of solvent caused a variable elemental analysis. Analytical data for **1** follow. ¹H NMR (300 MHz, C₆D₆, 25 °C) δ 0.882 (t, 18H, J = 7.171), 3.388 (q, 12H, J = 7.171), 7.238 (t, 3H, J = 7.150), 7.338 (t, 6H, J = 7.200), 7.838 (dd, 6H, J = 7.900, 1.300). ¹¹B NMR (96.205 MHz, C₆D₆, 25 °C) δ 50.628. Anal. Calcd for C₃₆H₅₉B₃N₆Mo₂: C, 54.03; H, 7.43; N, 10.50. Found: C, 54.98; H, 7.44; N, 10.11. Analytical data for **2** follow. ¹H NMR (300 MHz, C₆D₆, 25 °C) δ 1.071 (d, 36H, J = 6.681), 3.797 (sept, 6H, J = 6.554), 7.257 (t, 3H, J = 7.415), 7.377 (t, 6H, J = 7.577), 7.838 (dd, 6H, J = 6.903, 1.385). ¹¹B NMR (96.205 MHz, C₆D₆, 25 °C) δ 49.581. Anal. Calcd for C₃₆H₅₇B₃N₆Mo₂: C, 54.17; H, 7.20; N, 10.53. Found: C, 54.22; H, 7.09; N, 10.64.

W₂[RN–B^{Ph}–NR]₃, R = Et (3) and R = ⁱPr (4). Tetrahydrofuran solutions (7 mL) containing 100 mg of NaW₂Cl₇(THF)₅ were frozen. A suspension of PhB(EtNLi)₂·OEt₂ (79 mg) or a solution of PhB(ⁱPrNLi)₂ (65 mg) was added dropwise over 3 min to a partially thawed NaW₂Cl₇(THF)₅ solution. The mixture was allowed to slowly warm to room temperature. After the mixture stirred overnight, solvent was removed by vacuum evaporation, and 10 mL of pentane was added. The solution was filtered through Celite to remove LiCl. Concentration of the solution followed by cooling to –35 °C and finally filtration afforded 23 mg of tan crystals (25.8% crystal yield) of **3** and 22 mg of tan crystals (22.7% crystal yield) of **4**. Analytical data for **3** follow. ¹H NMR (300 MHz, C₆D₆, 25 °C) δ 0.969 (t, 18H, J = 7.000 Hz), 3.379 (q, 12H, J = 7.149 Hz), 7.2–7.4 (m, 9H), 7.604 (dd, 6H, J = 7.745, 1.192). ¹¹B NMR (96.205 MHz, C₆D₆, 25 °C) δ 51.937. Anal. Calcd for C₃₀H₄₅B₃N₆W₂: C, 40.49; H, 5.10; N, 9.44. Found: C, 40.63; H, 5.21; N, 9.36. Analytical data for **4** follow. ¹H NMR (300 MHz, C₆D₆, 25 °C) δ 1.145 (d, 36H, J = 6.681 Hz), 3.892 (sept, 6H, J = 6.518 Hz), 7.265 (t, 3H, J = 7.415 Hz), 7.383 (t, 6H, J = 7.252), 7.858 (dd, 6H, J = 7.985 Hz, 1.466 Hz). ¹¹B NMR (96.205 MHz, C₆D₆, 25 °C) δ 51.500. Anal. Calcd for C₃₆H₅₄B₃N₆W₂: C, 44.39; H, 5.90; N, 8.63. Found: C, 44.30; H, 5.76; N, 8.53.

Physical Methods. ¹H NMR spectra were recorded on solutions at 25 °C within the magnetic fields of a Varian Unity 300 or Mercury 300 spectrometers, which were located in the Department of Chemistry Instrumentation Facility (DCIF) at MIT. Chemical shifts are reported using the standard δ notation in ppm. ¹H spectra were referenced to residual solvent peak. ¹¹B{¹H} NMR spectra

- (18) Fest, D.; Habben, C. D.; Meller, A.; Sheldrick, G. M.; Stalke, D.; Pauer, F. *Chem. Ber.* **1990**, *123*, 703–706.
 (19) Habben, C. D.; Heine, A.; Sheldrick, G. M.; Stalke, D. *Z. Naturforsch.* **1992**, *47b*, 1367–1369.
 (20) Koch, H.-J.; Roesky, H. W.; Besser, S.; Herbst-Irmer, R. *Chem. Ber.* **1993**, *126*, 571–574.
 (21) Geschwentner, M.; Noltemeyer, M.; Elter, G.; Meller, A. *Z. Anorg. Allg. Chem.* **1994**, *620*, 1403–1408.
 (22) Chivers, T.; Gao, X.; Parvez, M. *Angew. Chem., Int. Ed. Engl.* **1995**, *34*, 2549–2551.
 (23) Albrecht, T.; Elter, G.; Noltemeyer, M.; Meller, A. *Z. Anorg. Allg. Chem.* **1998**, *624*, 1514–1518.
 (24) Manke, D. R.; Nocera, D. G. *Inorg. Chem.* **2003**, *42*, 4431–4436.
 (25) Manke, D. R.; Nocera, D. G. *Inorg. Chim. Acta* **2003**, *345*, 235–240.
 (26) Heine, A.; Fest, D.; Stalke, D.; Habben, C. D.; Meller, A.; Sheldrick, G. M. *J. Chem. Soc., Chem. Commun.* **1990**, 742–743.
 (27) Chivers, T.; Fedorchuk, C.; Schatte, G.; Parvez, M. *Inorg. Chem.* **2003**, *42*, 2084–2093.
 (28) Koch, H.-J.; Roesky, H. W.; Bohra, R.; Noltemeyer, M.; Schmidt, H.-G. *Angew. Chem., Int. Ed. Engl.* **1992**, *31*, 598–599.
 (29) Armarego, W. L. F.; Perrin, D. D. *Purification of Laboratory Chemicals*, 4th ed.; Butterworth-Heinemann: Oxford, 1996.
 (30) Gilbert, T. M.; Landes, A. M.; Rogers, R. D. *Inorg. Chem.* **1992**, *31*, 3438–3444.
 (31) Burch, J. E.; Gerrard, W.; Mooney, E. F. *J. Chem. Soc.* **1962**, 2200–2203.
 (32) Chisholm, M. H.; Eichhorn, B. W.; Folting, K.; Huffman, J. C.; Ontiveros, C. D.; Streib, W. E.; Van der Sluys, W. G. *Inorg. Chem.* **1987**, *26*, 3182–3186.

Table 1. Crystallographic Data for Mo₂[EtN–B^{Ph}–NEt]₃ (**1**) and W₂[ⁱPrN–B^{Ph}–NⁱPr]₃ (**4**)

	1	4
empirical formula	C ₃₆ H ₅₉ B ₃ Mo ₂ N ₆	C ₃₆ H ₅₇ B ₃ N ₆ W ₂
fw	800.2	974.01
<i>T</i> (K)	183(2)	193(2)
λ (Å)	0.71073 Å	0.71073 Å
space group	<i>P</i> 2 ₁ / <i>n</i>	<i>C</i> 2/ <i>c</i>
<i>a</i> (Å)	19.7976(14)	21.0389(13)
<i>b</i> (Å)	9.4329(6)	16.3854(10)
<i>c</i> (Å)	23.6392(16)	14.2619(9)
α (deg)	90	90
β (deg)	114.356(1)	126.897(1)
γ (deg)	90	90
<i>V</i> (Å ³)	4021.7(5)	3931.8(4)
<i>Z</i>	4	4
<i>d</i> _{calcd} (Mg/m ³)	1.322	1.645
abs coeff (mm ⁻¹)	0.655	5.879
R1 ^a	0.0457	0.0427
wR2 ^a	0.1222	0.1187

$$^a \text{R1} = \sum ||F_o| - |F_c|| / \sum |F_o|; \text{wR2} = [\sum w(F_o^2 - F_c^2)^2 / \sum w(F_o^2)^2]^{1/2}.$$

were collected at the DCIF on a Varian Unity 300 spectrometer and referenced to an external BF₃·OEt₂ standard at 0 ppm. UV–vis absorption spectra were collected on an Aviv 14DS spectrophotometer.

X-ray diffraction experiments were performed on single crystals grown from concentrated pentane or hexanes solutions at –35 °C. Crystals were removed from the supernatant liquid and transferred onto a microscope slide coated with Paratone N oil, and one was affixed to a glass fiber, coated in Paratone N oil, and cooled to –90 °C. Data collection was performed using the Mo K α (λ = 0.71073 Å) radiation of a Bruker CCD diffractometer. The data were processed and refined by using the program SAINT supplied by Siemens Industrial Automation, Inc. The structures were solved by direct methods (SHELXTL v6.10, Sheldrick, G. M., and Siemens Industrial Automation, Inc., 2000) in conjunction with standard difference Fourier techniques. All non-hydrogen atoms were refined anisotropically unless otherwise noted. Hydrogen atoms were placed in calculated positions. Two ethyl groups (C5 and C6, C7 and C8) in **1** were disordered over two sites. The disorder was modeled and refined to partial occupancy factors of 0.720230 for C5 and C6 (0.27977 for C5A and C6A) and 0.583690 for C7 and C8 (0.41631 for C7A and C8A). A *n*-hexane molecule was present in the asymmetric unit and was refined isotropically. DFIX instructions were used to set the distances in the disordered ethyl groups to those observed in the well-ordered groups, and to restrain the isotropically refined solvent molecule. Details regarding the refined data and cell parameters are provided in Table 1.

Computational Methods. Density functional theory (DFT) calculations were carried out at the local density approximation (LDA) level of theory using the Amsterdam Density Functional program.^{33–35} The calculations were performed on a home-built Linux cluster consisting of 60 processors running in parallel. Gradient corrections were introduced using the Becke exchange functional³⁶ (B) and the Lee–Yang–Parr³⁷ (LYP) correlation functional. Relativistic corrections were included by using the scalar zero-order regular approximation^{38–40} (ZORA). C and H were described by a Slater-type orbital triple- ξ basis set augmented by

one set of polarization functions. B, N, Mo, and W were described by a Slater-type orbital triple- ξ basis set augmented by two sets of polarization functions. Non-hydrogen atoms were assigned a relativistic frozen core potential, with the shells up to and including 3d for Mo, 4d for W, and 1s for B, C, and N treated as core.

Results and Discussion

Synthesis. The dilithio salts of bis(alkylamido)phenylboranes provide a useful reagent for the transfer of the bis-amido ligands to metal centers. The dilithio salts are prepared from the reaction of 2 equiv of *n*-BuLi with the corresponding diamine in greater than 90% yield. The ethyl derivative is isolated as the diethyl ether adduct. The ¹H NMR demonstrates two sets of ethyl peaks, one for the coordinated ether and one for the amido ethyl groups, that integrate equally. This NMR result is consistent with the elemental analysis, which indicates a single ether molecule per molecule of the dilithio salt. One set of ethyl resonances is well behaved, while the second exhibits a broad singlet for the methyl resonance. The isopropyl derivative is isolated solvent free and displays two isopropyl methyl resonances and a single methylene heptet in the ¹H NMR. A single resonance is observed in the ¹¹B NMR spectra of each of the salts.

Metathesis reactions between the dilithio salts of bis(alkylamido)phenylboranes with monomeric metal halides have proven effective in affording monomeric transition metal compounds of the diamido ligands.^{24,25} The reaction was employed here using Li₂[RN–B^{Ph}–NR] (R = Et, ⁱPr) with bimetallic metal halide starting materials “MoCl₃(dme)” or NaW₂Cl₇(THF)₅ to give tan and crystalline M₂[RN–B^{Ph}–NR]₃ compounds (M = Mo, R = Et (**1**) and ⁱPr (**2**); M = W, R = Et (**3**) and ⁱPr (**4**)) in yields of 23–25%. By ¹H NMR, all compounds in solution possess *D*_{3h} symmetry, with only single sets of ethyl and phenyl peaks observed for **1** and **3** and single sets of isopropyl and phenyl peaks observed for **2** and **4**; compounds **1**–**4** exhibit a single resonance in ¹¹B NMR spectra.

Structural Analysis. Crystals of **1** and **4** were analyzed by X-ray diffraction analysis. Both compounds possess three bis(alkylamido)phenylborane ligands spanning a metal–metal triple bond. Tables 2 and 3 list selected bond lengths and angles for compounds **1** and **4**, respectively. The solid-state structures exhibit pseudo-*D*_{3h} symmetry (Figure 1), which is consistent with the single set of alkyl resonances in the ¹H NMR spectra. These structures resemble the *D*_{3h} lantern structures reported by Cotton and co-workers for dimers of lesser bond order.^{41–43} The nearly eclipsed ligand

(33) *ADF2002.01*; SCM, Theoretical Chemistry, Vrije Universiteit: Amsterdam, The Netherlands, 2002.

(34) Fonseca Guerra, C.; Snijders, J. G.; Te Velde, G.; Baerends, E. J. *Theor. Chem. Acc.* **1998**, *99*, 391–403.

(35) Te Velde, G.; Bickelhaupt, F. M.; Baerends, E. J.; Fonseca Guerra, C.; Van Gisbergen, S. J. A.; Snijders, J. G.; Ziegler, T. *J. Comput. Chem.* **2001**, *22*, 931–967.

(36) Becke, A. D. *Phys. Rev. A* **1988**, *38*, 3098–3100.

(37) Lee, C.; Yang, W.; Parr, R. G. *Phys. Rev. B* **1988**, *37*, 785–789.

(38) Van Lenthe, E.; Baerends, E. J.; Snijders, J. G. *J. Chem. Phys.* **1993**, *99*, 4597–4610.

(39) Van Lenthe, E.; Baerends, E. J.; Snijders, J. G. *J. Chem. Phys.* **1994**, *101*, 9783–9792.

(40) Van Lenthe, E.; Ehlers, A.; Baerends, E. J. *J. Chem. Phys.* **1999**, *110*, 8943–8953.

(41) Cotton, F. A.; Daniels, L. M.; Falvello, L. R.; Murillo, C. A. *Inorg. Chim. Acta* **1994**, *219*, 7–10.

(42) Cotton, F. A.; Daniels, L. M.; Maloney, D. J.; Murillo, C. A. *Inorg. Chim. Acta* **1996**, *249*, 9–11.

(43) Cotton, F. A.; Daniels, L. M.; Falvello, L. R.; Matonic, J. H.; Murillo, C. A. *Inorg. Chim. Acta* **1997**, *256*, 269–275.

Table 2. Selected Bond Lengths (Å) and Angles (deg) for $Mo_2[EtN-B^{Ph}-NEt]_3$ (**1**)

Bond Lengths			
Mo(1)–Mo(2)	2.1612(6)	N(1)–B(1)	1.444(7)
Mo(1)–N(2)	1.983(4)	N(2)–B(1)	1.438(7)
Mo(1)–N(4)	1.990(4)	N(3)–B(2)	1.429(7)
Mo(1)–N(6)	1.975(4)	N(4)–B(2)	1.452(7)
Mo(1)–N(1)	1.980(4)	N(5)–B(3)	1.440(7)
Mo(1)–N(3)	2.002(4)	N(6)–B(3)	1.437(7)
Mo(1)–N(5)	1.975(4)		
Bond Angles			
Mo(1)–Mo(2)–N(1)	94.56(12)	Mo(1)–N(6)–C(11)	119.8(3)
Mo(1)–Mo(2)–N(3)	94.26(11)	Mo(2)–N(1)–C(1)	119.4(3)
Mo(1)–Mo(2)–N(4)	94.35(12)	Mo(2)–N(3)–C(5)	125.8(4)
Mo(2)–Mo(1)–N(4)	94.12(11)	Mo(2)–N(5)–C(9)	119.6(3)
Mo(2)–Mo(1)–N(5)	94.57(12)	Mo(1)–N(2)–B(1)	117.0(3)
Mo(2)–Mo(1)–N(6)	94.21(11)	Mo(1)–N(4)–B(2)	116.4(3)
N(1)–B(1)–N(2)	117.0(3)	Mo(1)–N(6)–B(3)	117.0(3)
N(3)–B(2)–N(4)	117.9(5)	Mo(2)–N(1)–B(1)	116.6(3)
N(5)–B(3)–N(6)	117.3(5)	Mo(2)–N(3)–B(2)	116.7(3)
Mo(1)–N(2)–C(3)	119.3(3)	Mo(2)–N(5)–B(3)	116.9(3)
Mo(1)–N(4)–C(7)	124.0(4)		
Torsion Angles			
N(1)–Mo(2)–Mo(1)–N(2)	0.2	N(3)–Mo(2)–Mo(1)–N(2)	122.0
N(3)–Mo(2)–Mo(1)–N(4)	0.4	N(3)–Mo(2)–Mo(1)–N(6)	119.9
N(5)–Mo(2)–Mo(1)–N(6)	1.3	N(5)–Mo(2)–Mo(1)–N(2)	116.8
N(1)–Mo(2)–Mo(1)–N(4)	121.4	N(5)–Mo(2)–Mo(1)–N(4)	121.6
N(1)–Mo(2)–Mo(1)–N(6)	118.3		

Table 3. Selected Bond Lengths (Å) and Angles (deg) of $W_2[PrN-B^{Ph}-N^iPr]_3$ (**4**)

Bond Lengths			
W(1)–W(1A)	2.2351(7)	N(1)–B(1A)	1.436(13)
W(1)–N(1)	1.984(7)	N(2)–B(1)	1.468(13)
W(1)–N(2)	1.985(7)	N(3)–B(2)	1.456(10)
W(1)–N(3)	1.959(8)		
Bond Angles			
N(1)–W(1)–W(1A)	93.1(2)	W(1)–N(1)–B(1A)	114.6(6)
N(2)–W(1)–W(1A)	94.2(2)	W(1)–N(2)–B(1)	113.0(6)
N(3)–W(1)–W(1A)	94.0(2)	W(1)–N(3)–B(2)	116.6(7)
W(1)–N(1)–C(1)	124.9(6)	N(1A)–B(1)–N(2)	118.0(8)
W(1)–N(2)–C(4)	118.2(6)	N(3)–B(2)–N(3A)	118.8(12)
W(1)–N(3)–C(7)	123.8(6)		
Torsion Angles			
N(1)–W(1)–W(1A)–N(2A)	0.4	N(1)–W(1)–W(1A)–N(3A)	120.7
N(3)–W(1)–W(1A)–N(3A)	1.6	N(2)–W(1)–W(1A)–N(2A)	116.0
N(1)–W(1)–W(1A)–N(1A)	116.7		

geometry is most directly indicated by the N–M–M–N torsion angles, which are only 0.2–1.6°. The coordination geometry of each metal center is nearly trigonal pyramidal, as demonstrated by M–M–N angles of 93.1(2)–94.57(12)°. In the bridging mode observed here, metric parameters of the bis(alkylamido)phenylborane ligands are similar to those when the ligands chelate a metal center.^{18,24,25} The N–B distances of 1.429(7)–1.468(13) Å indicate significant N–B π -bonding. The only exceptional difference for the ligands in chelating versus bridging modes is the N–B–N angle, which increases from 110.4(3)–111.2(4)° to 117.0(3)–118.8(12)°, respectively.

As is usually the case for metal–metal dimers, the most intriguing metric is the metal–metal bond distance. The values of 2.1612(6) and 2.2351(7) Å for **1** and **4**, respectively, are exceptional. The shortest M–M distances observed for M_2X_6 species prior to this study were 2.167 Å (Mo)⁴⁴ and 2.255 Å (W).⁴⁵

The steric constraints imposed by the three-atom N–B–N bridge appear to be the determinant factor in the short metal–metal bond lengths and small torsional distortion of **1**–**4**. The only previous d^3 – d^3 molybdenum dimer with a three-atom bridge, $Mo_2[O_2Si(O^tBu)_2]_3$, possesses an average X–M–M–X torsion angle of 3°, an angle that is more than twice that observed for **1**. The major structural differences between the two three-atom backbones are highlighted in Figure 2. The trigonal boron produces an average N–B–N angle of 117.4°, whereas the tetrahedral silicon produces an average O–Si–O angle of 105.4°. In conjunction with the longer Si–O bond, as compared to that of N–B, the average O···O separation of the disiloxide bridged complex is longer (2.616 Å) than the N···N separation in **1** (2.461 Å). The more constrained five-membered $\overline{M-N-B-N-M}$ ring accounts for its greater planarity and shorter M–M bond of **1**. The M–M bonds of **1** and **4** are also significantly shorter than their staggered bis(amide) analogues and than all other monodentate anionic ligands (Table 4).^{46–49} The contraction in M–M distance of 0.05–0.06 Å is greater than that observed between molybdenum and tungsten compounds possessing four-atom bridging ligands and their unbridged counterparts ($\Delta d = -0.02$ Å). It is also noteworthy that the M–M distance in the bridging disiloxide complex is longer than its unbridged alkoxide analogues. We attribute this disparity between **1** and $Mo_2[O_2Si(O^tBu)_2]_3$ to the longer O···O separation (owing to the longer $d(Si-O)$). That both complexes possess nearly eclipsed torsional conformations suggests that the short metal–metal bond of **1** is of steric and not of electronic origin.

Electronic Structure. Density functional calculations were performed on model molybdenum and tungsten compounds, in which methyl groups substitute for alkyl substituents and the geometry of a $M_2[MeN-B^{Ph}-NMe]_3$ is constrained to D_{3h} symmetry. Agreement between calculated and observed structures suggests that these simplifications are reasonable. A geometry optimization yielded metal–metal bond distances that are about 0.1 Å different from the crystallographic data ($d(Mo-Mo) = 2.17342$ Å; $d(W-W) = 2.24728$ Å).

Figure 3 displays the energy levels and representations of the frontier Kohn–Sham molecular orbitals. We note that Kohn–Sham orbitals differ from those derived from a Hartree–Fock (HF) formalism by the inclusion of the exchange–correlation energy;⁵⁰ however, comparative analysis establishes that the shapes and symmetries of the Kohn–Sham orbitals accord well with those calculated by more

(44) Huq, F.; Mowat, W.; Shortland, A.; Skapski, A. C.; Wilkinson, G. J. *Chem. Soc., Chem. Commun.* **1971**, 1079–1080.

(45) Chisholm, M. H.; Cotton, F. A.; Extine, M.; Stults, B. R. *Inorg. Chem.* **1976**, *15*, 2252–2257.

(46) Chisholm, M. H.; Cotton, F. A.; Frenz, B. A.; Reichert, W. W.; Shive, L. W.; Stults, B. R. *J. Am. Chem. Soc.* **1976**, *98*, 4469–4476.

(47) Cotton, F. A.; Stults, B. R.; Troup, J. M.; Chisholm, M. H.; Extine, M. J. *Am. Chem. Soc.* **1975**, *97*, 1242–1243.

(48) Chisholm, M. H.; Cotton, F. A.; Murillo, C. A.; Reichert, W. W. *Inorg. Chem.* **1977**, *16*, 1801–1808.

(49) Chisholm, M. H.; Clark, D. L.; Folting, K.; Huffman, J. C.; Hampden-Smith, M. J. *Am. Chem. Soc.* **1987**, *109*, 7750–7761.

(50) Kohn, W.; Becke, A. D.; Parr, R. G. *J. Phys. Chem.* **1996**, *100*, 12974–12980.

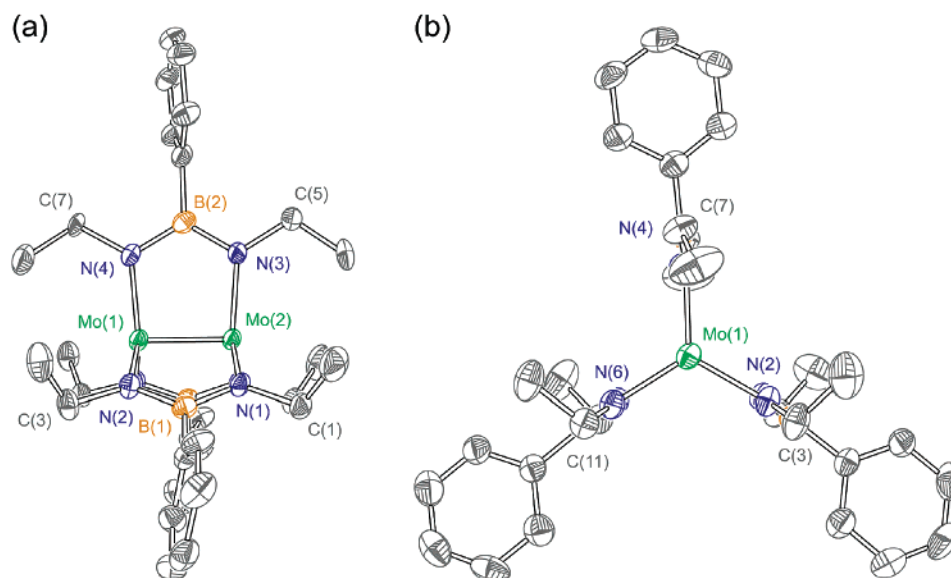


Figure 1. Solid-state structure of $\text{Mo}_2[\text{EtN}-\text{B}^{\text{Ph}}-\text{NEt}]_3$ (**1**) viewed (a) normal to and (b) along the metal–metal axis with thermal ellipsoids shown at the 30% probability level.

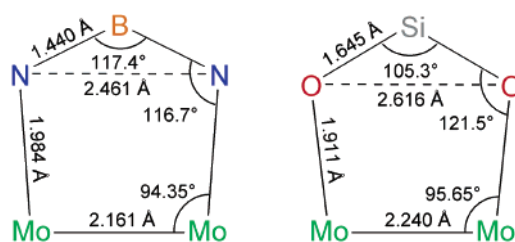


Figure 2. Geometrical comparison of the two known three-atom bridged d^3-d^3 dimolybdenum complexes, $\text{Mo}_2[\text{EtN}-\text{B}^{\text{Ph}}-\text{NEt}]_3$ (**1**) and $\text{Mo}_2[\text{O}_2\text{Si}(\text{O}^t\text{Bu})_2]_3$.

Table 4. Metal–Metal Triple Bond Lengths of Eclipsed and Staggered M_2X_6 Complexes

$d(\text{Mo}\equiv\text{Mo})/\text{Å}$		$d(\text{W}\equiv\text{W})/\text{Å}$	
$\text{Mo}_2(\text{NMe}_2)_6^a$	2.211(2)	$\text{W}_2(\text{NMe}_2)_6^s$	2.294(1)
$\text{Mo}_2(\text{DMEDA})_3^b$	2.190(1)	$\text{W}_2(\text{DMEDA})_3^h$	2.265(1)
$\text{Mo}_2(\text{OCH}_2\text{CMe}_3)_6^c$	2.222(2)	$\text{W}_2(\text{O}^i\text{Pr})_6^i$	2.315(2)
$\text{Mo}_2(\text{OCMe}_2\text{CMe}_2\text{O})_3^d$	2.1942(6)	$\text{W}_2(\text{OCMe}_2\text{CMe}_2\text{O})_3^j$	2.2738(8)
$\text{Mo}_2(\text{O}_2\text{Si}(\text{O}^t\text{Bu})_2)_3^e$	2.240(1)		
$\text{Mo}_2(\text{CH}_2\text{SiMe}_3)_6^f$	2.167	$\text{W}_2(\text{CH}_2\text{SiMe}_3)_6^k$	2.255(2)
$\text{Mo}_2[\text{EtN}-\text{B}^{\text{Ph}}-\text{NEt}]_3$	2.1612(6)	$\text{W}_2[\text{PrN}-\text{B}^{\text{Ph}}-\text{N}^i\text{Pr}]_3$	2.2351(7)

^a Reference 46. ^b Reference 7. ^c Reference 48. ^d Reference 8. ^e Reference 12. ^f Reference 44. ^g Reference 47. ^h Reference 9. ⁱ Reference 49. ^j Reference 11. ^k Reference 45.

traditional HF and extended Hückel approximations,^{51,52} and indeed, these orbitals have found widespread use in electronic structure descriptions.^{53–59} In both complexes, the HOMO is a nitrogen p based orbital, similar to the result obtained

for $\text{Mo}_2(\text{NMe}_2)_6$.^{4,5} Metal–metal character is first observed in the HOMO – 1 for the molybdenum complex and in HOMO – 2 for the tungsten complex; for the latter, another set of nitrogen p based orbitals lies between it and the HOMO. The LUMO for the molybdenum dimer is δ bonding, with the Mo–Mo π^* orbital lying immediately to higher energy. For the tungsten case, the δ and π^* orbitals are displaced to higher energy, and a W–W σ^* orbital assumes the LUMO position; this σ^* orbital for the molybdenum complex is LUMO + 2. Large HOMO–LUMO gaps of 3.1848 and 3.2031 eV are observed for dimolybdenum and ditungsten complexes, respectively. The $d\sigma$ and $d\pi$ of ML_3 orbitals do not exhibit significant rehybridization, and no obvious orbital or orbital set of the ML_3 fragments appears to lead to enhanced orbital overlap in an eclipsed ligand configuration.

The large HOMO–LUMO gap is manifested in the absorption spectra of the $\text{M}_2[\text{RN}-\text{B}^{\text{Ph}}-\text{NR}]_3$ complexes. The absorption profile of **1** and **2** are dominated by a single, intense band at 310 nm. A similar feature is observed in the absorption spectrum of $\text{Mo}_2(\text{NMe}_2)_6$, and it has been ascribed to a LMCT transition. The appearance of the LMCT transition of $\text{Mo}_2(\text{NMe}_2)_6$ to slightly lower energy ($\lambda_{\text{max}} = 325$ nm) is consistent with the longer Mo–Mo bond of the unbridged dimer.⁶⁰ The allowed metal-based $\pi \rightarrow \pi^*$ transition of the molybdenum dimer is believed to be masked by the LMCT absorption. The LMCT transition shifts to significantly higher energy for ditungsten complexes. In $\text{W}_2(\text{NMe}_2)_6$, the LMCT shifts to $\lambda_{\text{max}} = 282$, revealing the $\pi \rightarrow \pi^*$ transition as a shoulder ($\lambda_{\text{max}} = 360$ nm) on the

- (51) Stowasser, R.; Hoffmann, R. *J. Am. Chem. Soc.* **1999**, *121*, 3414–3420.
 (52) Hamel, S.; Duffy, P.; Casida, M. E.; Salahub, D. R. *J. Electron Spectrosc.* **2002**, *123*, 345–363.
 (53) Lehnert, N.; Neese, F.; Ho, R. Y. N.; Que, L., Jr.; Solomon, E. I. *J. Am. Chem. Soc.* **2002**, *124*, 10810–10822.
 (54) Chen, P.; Root, D. E.; Campochiaro, C.; Fujisawa, K.; Solomon, E. I. *J. Am. Chem. Soc.* **2003**, *125*, 466–474.
 (55) Chisholm, M. H.; Gallucci, J.; Hadad, C. M.; Huffman, J. C.; Wilson, P. J. *J. Am. Chem. Soc.* **2003**, *125*, 16040–16049.
 (56) Gray, T. G.; Rudzinski, C. M.; Meyer, E.; Holm, R. H.; Nocera, D. G. *J. Am. Chem. Soc.* **2003**, *125*, 4755–4770.

- (57) Bachmann, J.; Nocera, D. G. *J. Am. Chem. Soc.* **2004**, *126*, 2829–2837.
 (58) Gray, T. G.; Rudzinski, C. M.; Meyer, E. E.; Nocera, D. G. *J. Phys. Chem. A* **2004**, *108*, 3238–3243.
 (59) Gray, T. G.; Veige, A. S.; Nocera, D. G. *J. Am. Chem. Soc.*, accepted for publication.
 (60) Chisholm, M. H.; Clark, D. L.; Kober, E. M.; Van Der Sluys, W. G. *Polyhedron* **1987**, *6*, 723–727.

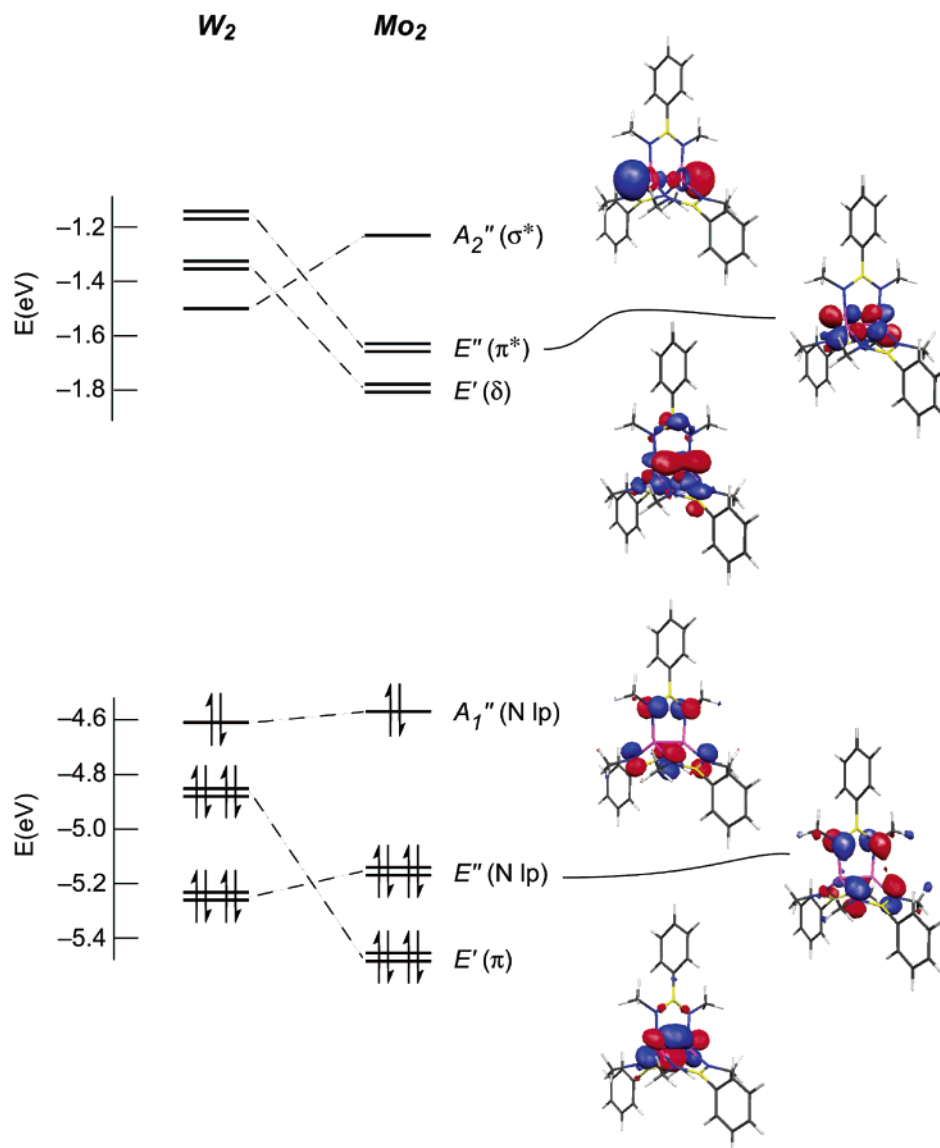


Figure 3. Calculated frontier orbitals of model compounds $Mo_2[MeN-B^{Ph}-NMe]_3$ and $W_2[MeN-B^{Ph}-NMe]_3$.

trailing edge of the charge-transfer absorption band. A similar profile is observed for ditungsten complexes **3** and **4**. As with the dimolybdenum complex, these absorption bands are blue-shifted ($\lambda_{max} = 271$ and 334 nm) relative to the unbridged $W_2(NMe_2)_6$ dimer.

The chemical properties of the $M_2[RN-B^{Ph}-NR]_3$ complexes are consistent with the electronic structure of Figure 4. The ligand-based HOMO and high energy of the LUMO preclude an inert reaction chemistry; this is the case. The complexes do not react with σ -donor ligands nor do they react with oxo and chalcogenide transfer reagents (e.g., nitriles, ketones, epoxides, pyridine *N*-oxide, selenium). The complexes are, however, susceptible to oxidation, as indicated by their pyrophoric nature when exposed to air.

The $M_2[RN-B^{Ph}-NR]_3$ complexes reported herein expand the transition metal chemistry of bis(alkylamido)boranes from mononuclear centers to bimetallic cores. The compounds are complementary to those bimetallic cores that are spanned by ligands composed of three-atom bridges in which two π -accepting groups (e.g., fluorophosphines) are adjacent to

a donor bridgehead (e.g., amine). We have shown that this A–D–A ligand motif supports bimetallic cores in a two-electron mixed valence configuration.^{59–66} We describe herein bimetallic centers of the transition metal series spanned by a ligand of antithetical composition: a D–A–D three-atom frame composed of a π -accepting boron bridgehead adjacent to π -donor amides. This D–A–D backbone is very constrained, thus affording compounds with exceptional properties for the class of triple metal–metal bond complexes.

Acknowledgment. This work was supported by a grant from the National Science Foundation (CHE-0132680).

(61) Heyduk, A. F.; Macintosh, A. M.; Nocera, D. G. *J. Am. Chem. Soc.* **1999**, *121*, 5023–5032.

(62) Odom, A. L.; Heyduk, A. F.; Nocera, D. G. *Inorg. Chim. Acta* **2000**, *297*, 330–337.

(63) Heyduk, A. F.; Nocera, D. G. *J. Am. Chem. Soc.* **2000**, *122*, 9415–9426.

(64) Heyduk, A. F.; Nocera, D. G. *Chem. Commun.* **1999**, 1519–1520.

(65) Heyduk, A. F.; Nocera, D. G. *Science* **2001**, *293*, 1639–1641.

(66) Veige, A. S.; Nocera, D. G. *Chem. Commun.*, accepted for publication.

Supporting Information Available: Table of X-ray crystallographic data for complexes **1** and **4** including a fully labeled thermal ellipsoid plot, final atomic coordinates, equivalent isotropic displacement parameters, anisotropic displacement parameters, and

bond distances and angles. This material is available free of charge via the Internet at <http://pubs.acs.org>.

IC049795R